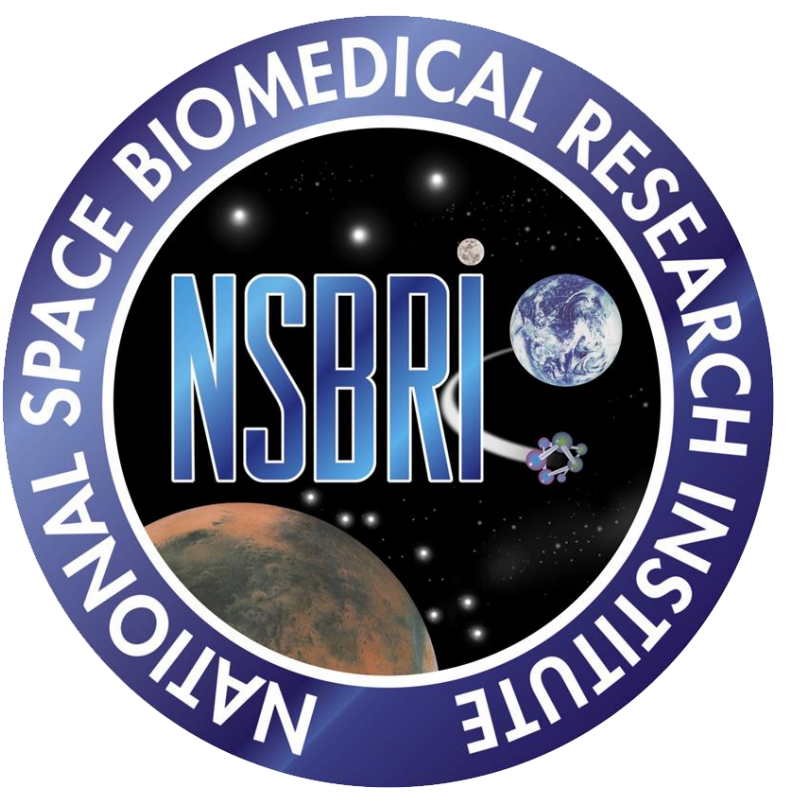


# Structural and Effective Material Properties of the Anterior, Lateral, and Posterior Human Rib Bone



Taylor L. Comte<sup>1</sup>, Matthew W. Kindig<sup>2</sup>, Anthony G. Lau<sup>1,2</sup>

<sup>1</sup>University of North Carolina at Chapel Hill- Biomedical Engineering, <sup>2</sup>University of Virginia-Center for Applied Biomechanics

## Introduction

Thoracic Injuries: 2<sup>nd</sup> to head injuries in number of fatalities and serious injuries in vehicle crashes.

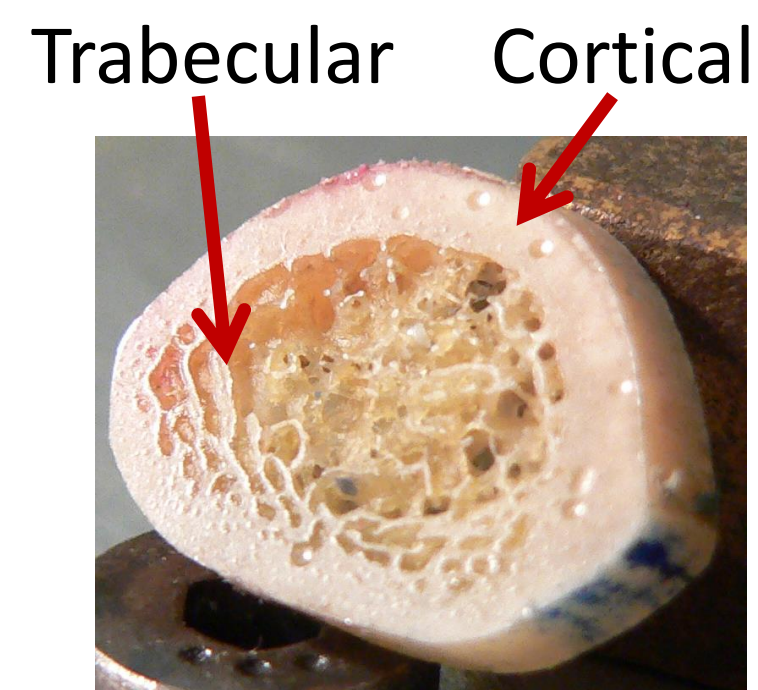
Finite Element (FE) simulations approximate frontal impacts on rib fracture rate.

Currently, ribs are modeled as **solid** and **HOMOGENOUS** structures.

With elastic modulus based on tensile coupon tests.

However, rib bone is porous.

This study proposes an elastic modulus based on **MicroCT** images and simulations performed with microstructurally correct **FE models**.



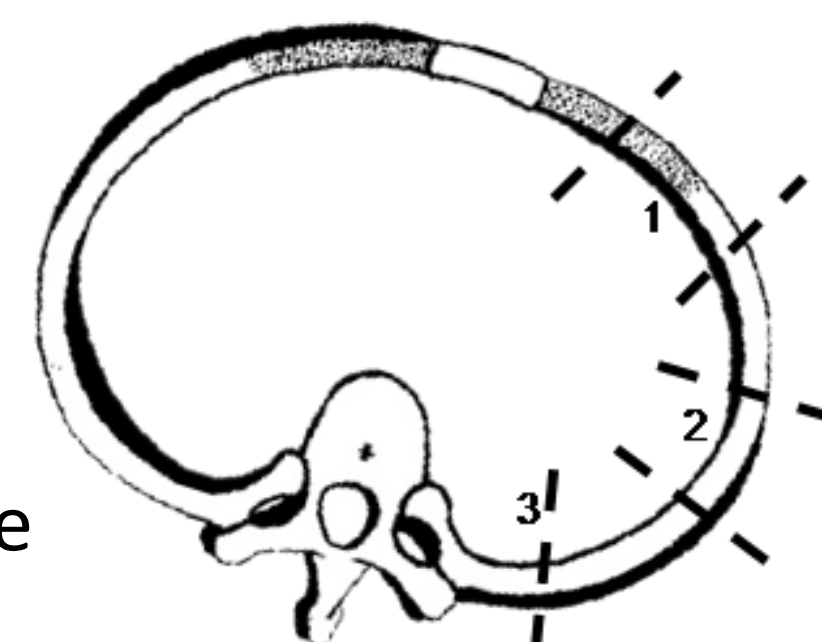
Rib bone showing cortical (compact) outer region, and trabecular (porous) inner region.

## Methods

### Study Design:

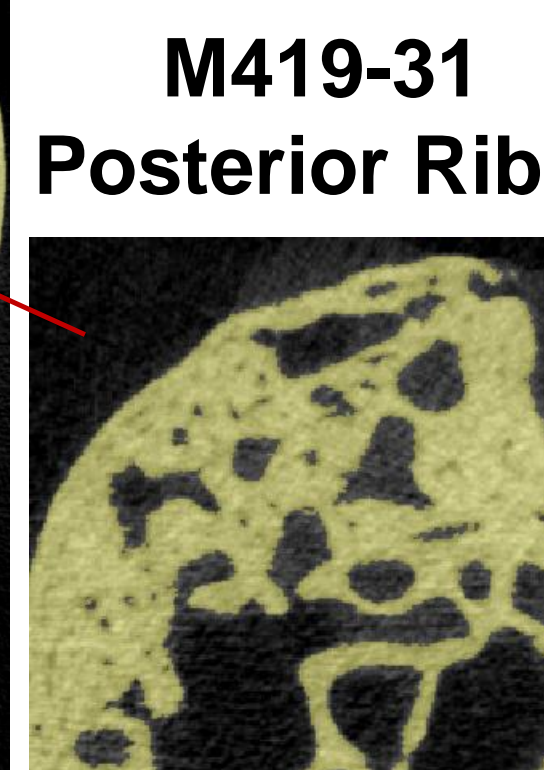
	Cadaver 1	Cadaver 2	Cadaver 3
Gender	Male	Male	Male
PMHS ID	412	413	419
Age	62	54	31
Name	M412-62	M413-54	M419-31

1.0mm thick cross sections were dissected from ribs 1-7 at anterior (1), lateral (2), and posterior (3) positions (right).

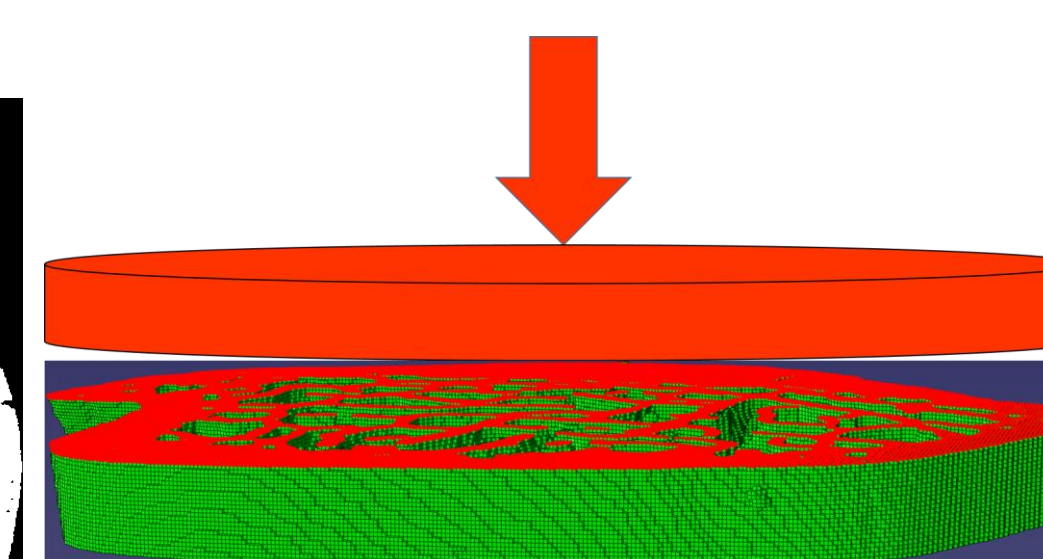
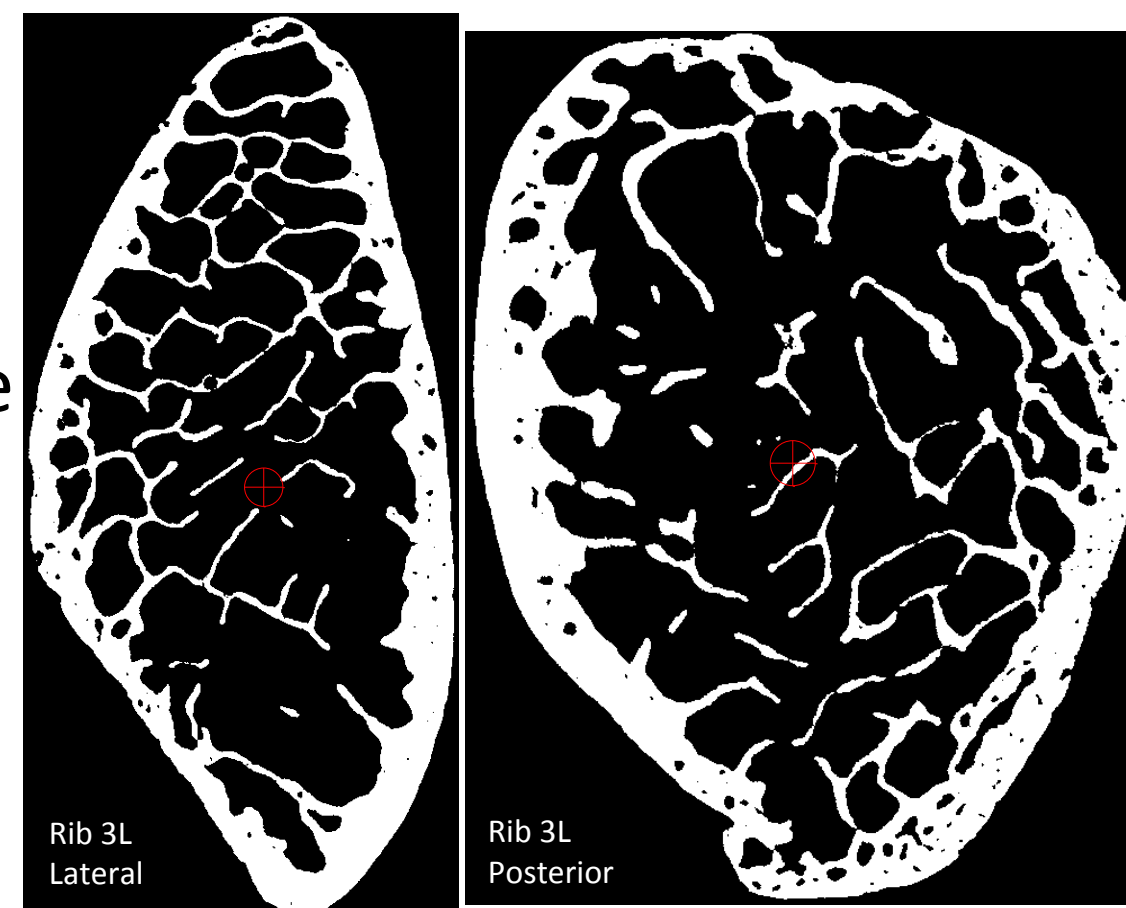


### Imaging Techniques

- MicroCT scans were taken at 15µm.
- Images were segmented with MIMICS 16.0 (left) by selecting voxel intensities ≥4100HU (or 600mgHA/cc).
- ABAQUS CAE 6.9 was used for Finite Element Analysis. Bone material properties were assumed to be homogenous ( $E=13.9$  GPa,  $\nu=0.3$ ).



**Polar Moment of Inertia:** A custom Matlab script was developed to determine the geometric centroid (right) and the polar moment of inertia of each rib cross section

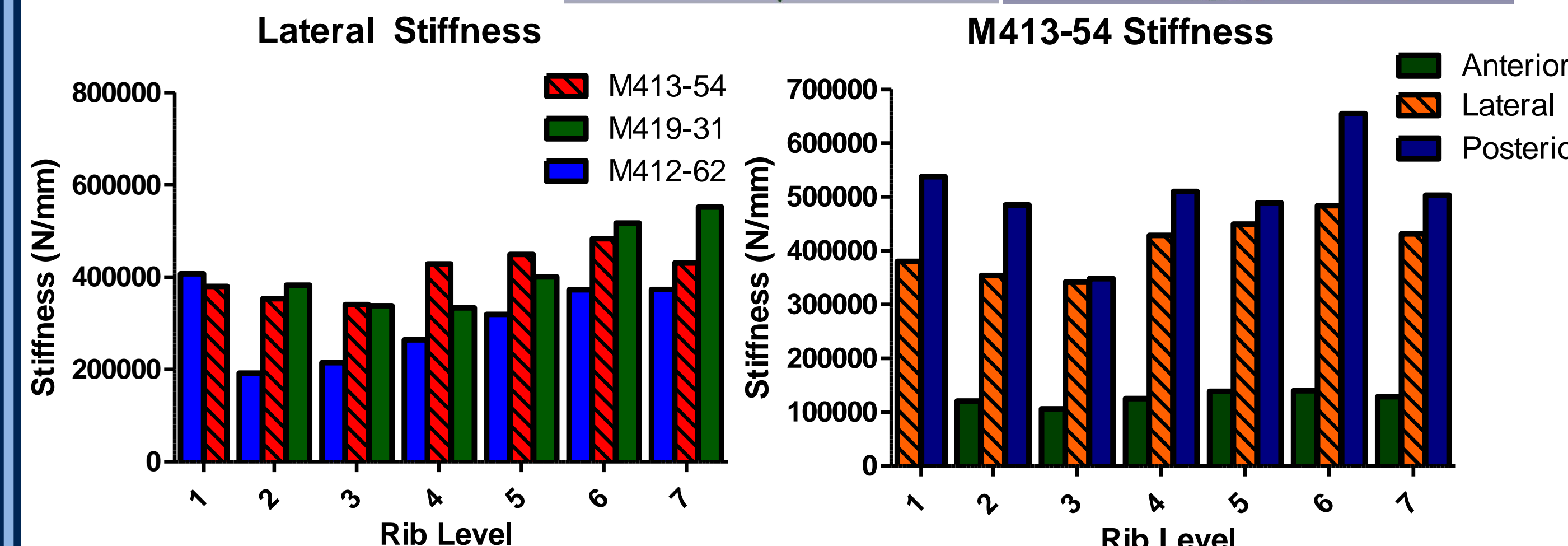
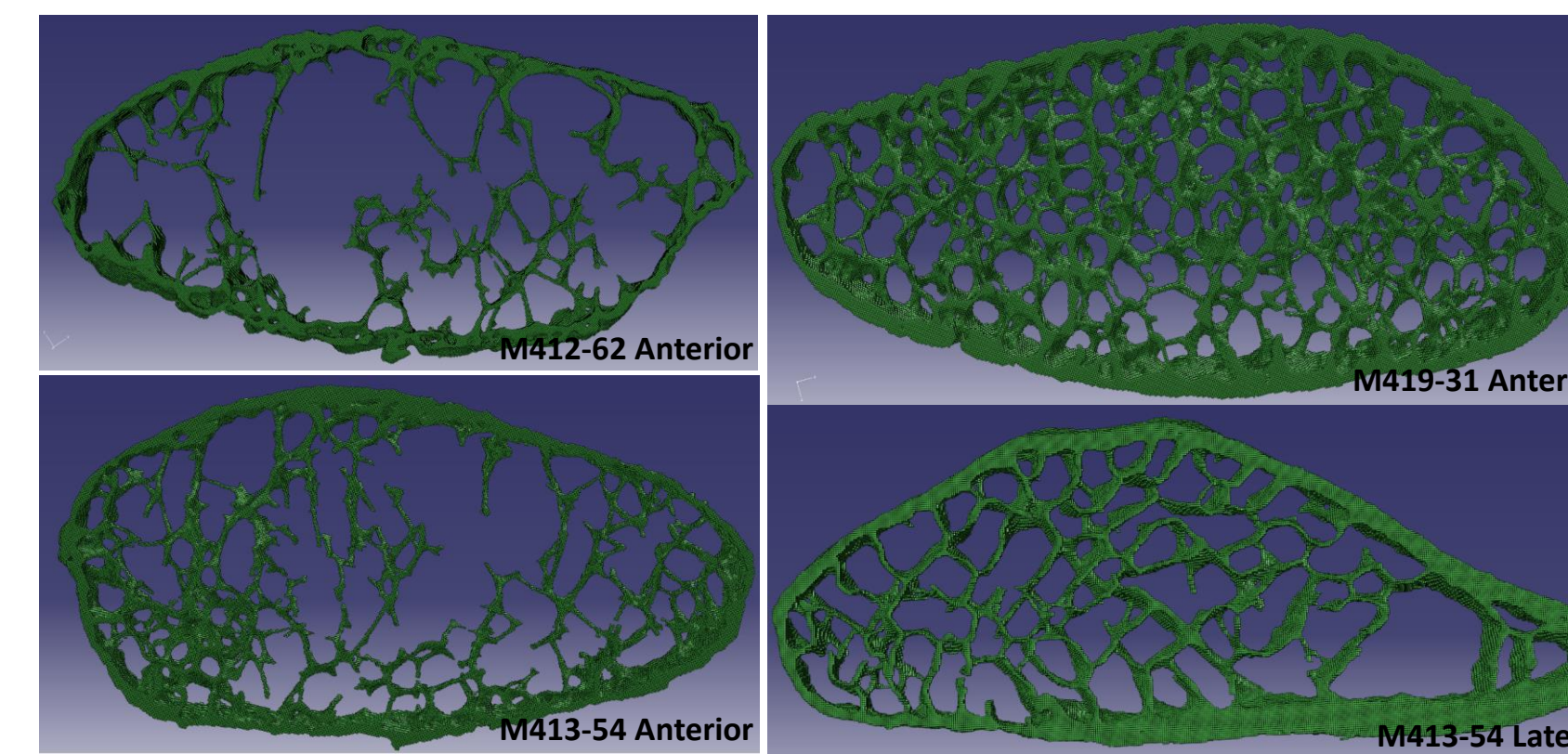


Bone stiffness was calculated as the resultant force (N) from the applied displacement (5 µm) (above).

## Results

### Rib Stiffness:

- Stiffest: Cadaver M419-31
- Least Stiff: Cadaver 412-62



General trend for bone volume and stiffness: decline to rib 3 and increase from rib 4 to rib 7.

Posterior ribs were the stiffest followed by lateral, and anterior ribs. (Left).

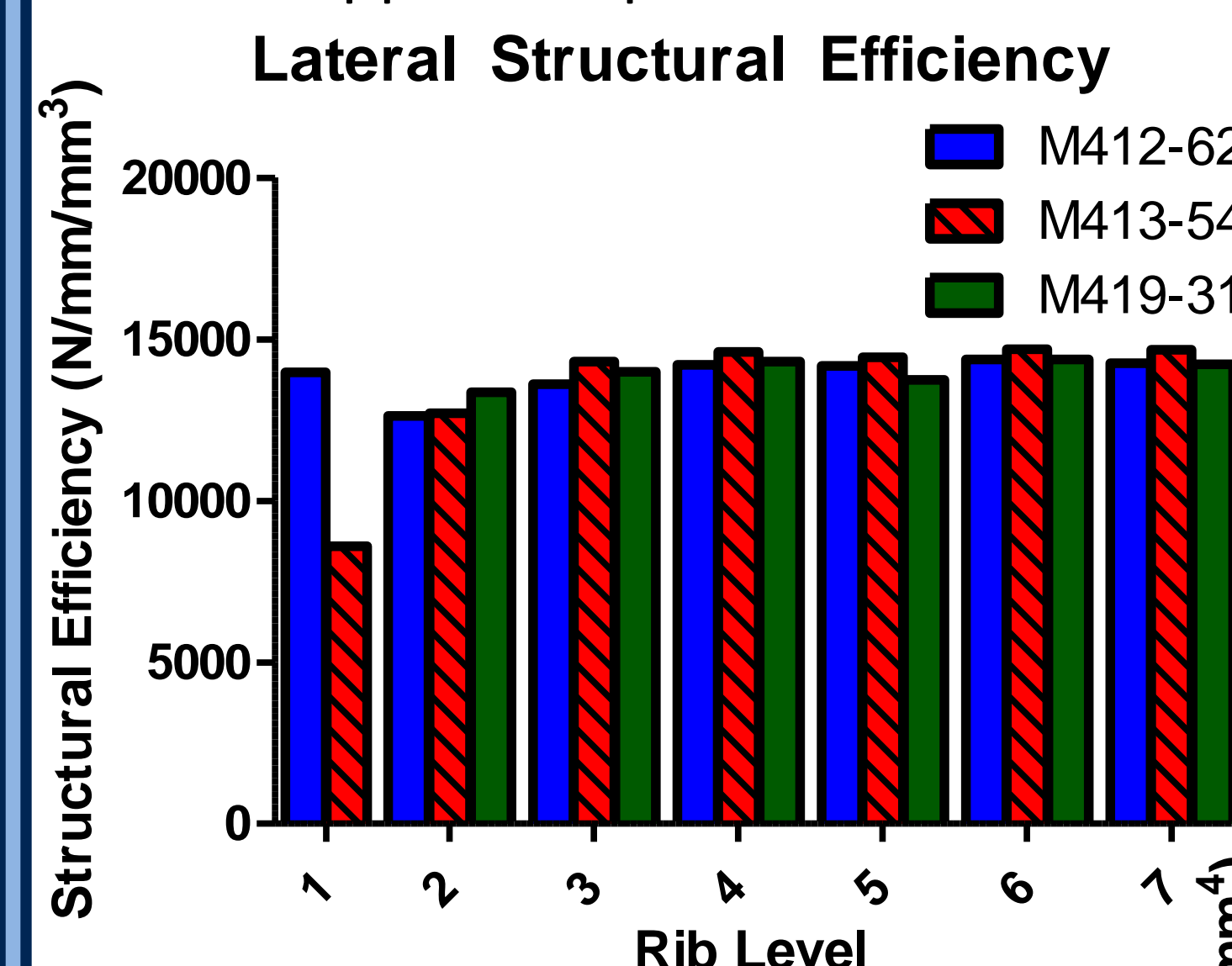
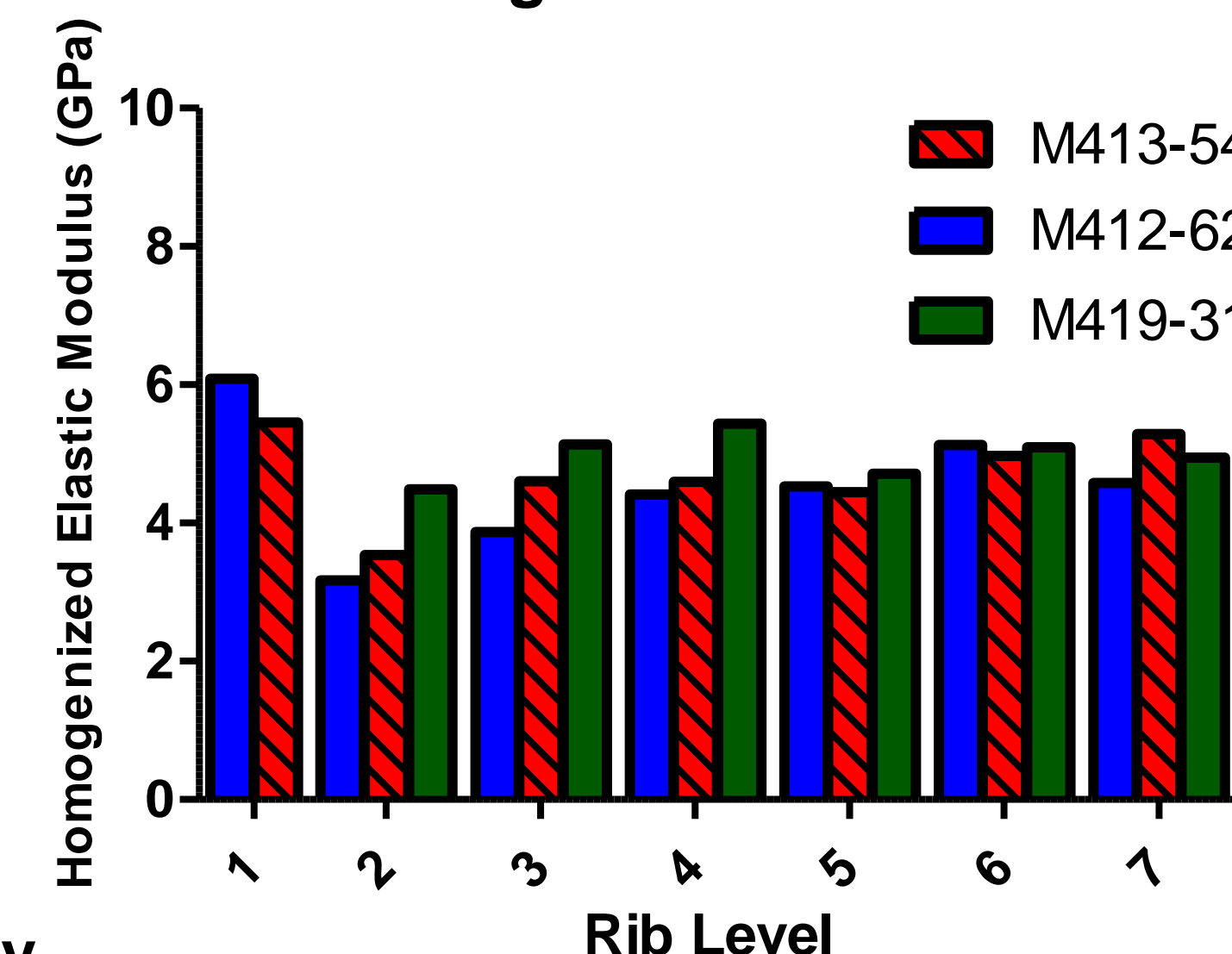
### Homogenized Elastic Modulus:

Anterior ribs: 1.0-2.2GPa  
Lateral ribs: 3.2-6.1GPa  
Posterior ribs: 4.6-8.0GPa

$$E = \frac{\sigma}{\epsilon} \quad \sigma = \frac{F}{A} \quad \epsilon = \frac{\Delta L}{L}$$

Force (F) from FE simulation  
Area (A) of 1<sup>st</sup> DICOM slice with pores filled in (total cross sectional area of rib)  
 $\epsilon$  from applied displacement

### Lateral Homogenized Elastic Modulus



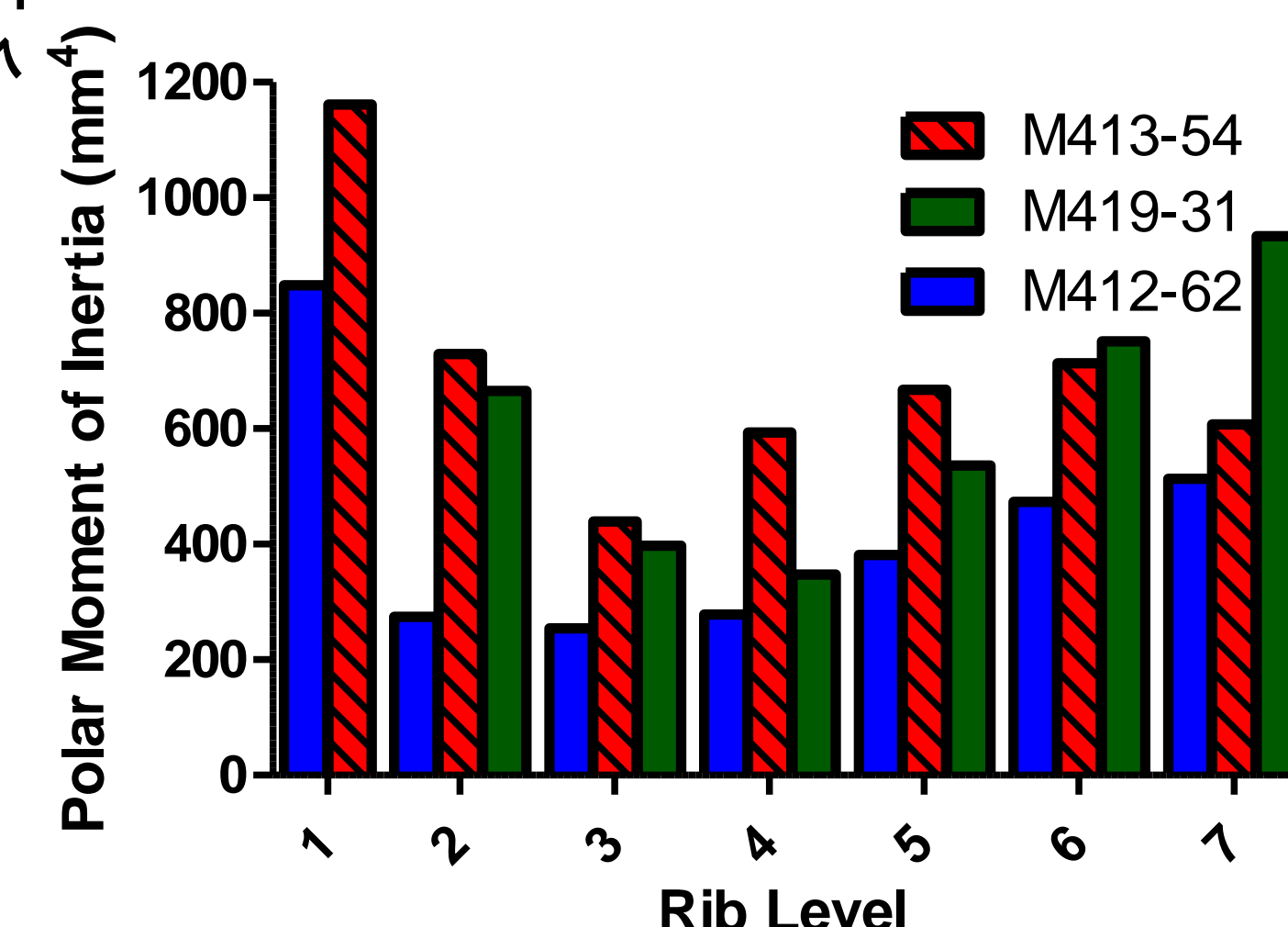
### Polar Moment of Inertia:

- Trend: decline to ribs 3 or 4 and increase from rib 5-7.
- Rib 1 generally had greatest moment of inertia.
- Cadaver M412-62 had ribs with lowest moment of inertia.

### Bone Structural Efficiency (Stiffness/Bone Volume):

Average structural efficiency was 14100±400N/mm/mm<sup>3</sup>.

### Lateral Polar Moment of Inertia



## Discussion

### Structural Properties:

The general trend in bone volume, stiffness, and polar moment of inertia for lateral and posterior ribs was to decline to rib 3 or 4, and increase from rib 4 to 7. The oldest cadaver (M412-62) generally had the lowest value for all structural properties analyzed, except structural efficiency. The anterior rib sections had much lower results in all the structural properties, including structural efficiency.

Overall, the youngest cadaver (M419-31) had the most bone volume in the lateral (38.82mm<sup>3</sup>) and posterior regions (47.48mm<sup>3</sup>) at rib 7. Inspection of the cadavers separately revealed Rib 1 to have the most bone volume in the lateral position for both M412-62 (29.17mm<sup>3</sup>) and M413-54 (44.2mm<sup>3</sup>). The average bone volume for anterior ribs (14±5mm<sup>3</sup>) was less than lateral (28±7mm<sup>3</sup>) and posterior ribs (33±6mm<sup>3</sup>).

Rib 7 of the youngest cadaver was the stiffest overall in lateral and posterior positions. Ribs of the oldest cadaver (M412-62) were consistently lowest in stiffness. The youngest cadaver (M419-31) had greater stiffness in the anterior ribs compared to M413-54 (36±9%).

Structural efficiency was similar among the lateral and posterior ribs of all 3 cadavers and at all rib levels (14100±400N/mm/mm<sup>3</sup>). The anterior ribs were much lower in structural efficiency (9600±500N/mm/mm<sup>3</sup>).

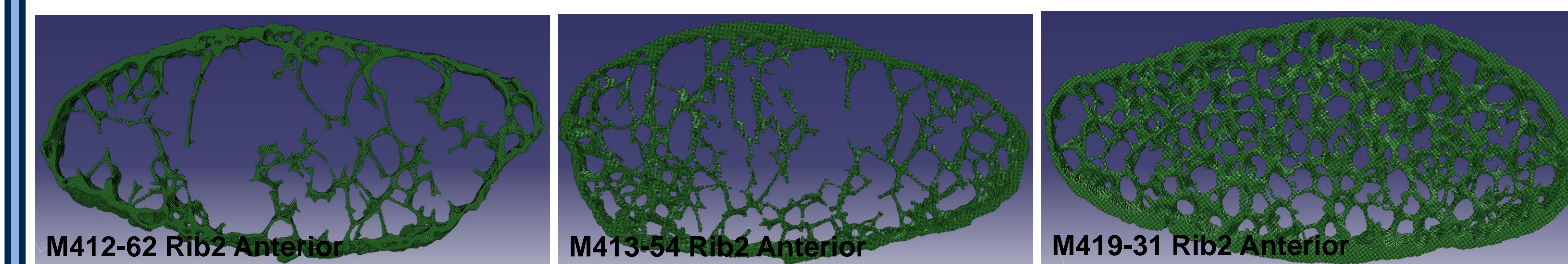
Polar moment of inertia was greatest in ribs 1 and 7 of the youngest cadaver (M419-31), and was consistently lowest for the oldest cadaver (M412-62).

### Material Properties:

Elastic Modulus was greatest for posterior ribs (6.4±1.0GPa), followed by lateral (4.7±.7GPa) and anterior (1.6±.4GPa) ribs. Overall the homogenized elastic modulus was less sensitive to differences between cadavers and rib levels compared to structural properties.

### Study Limitations:

The material properties of the anterior ribs could be affected by costal cartilage calcifications that are more prevalent in older individuals. It is also important to note the high porosity of the anterior ribs. The number of cadavers used in this study were an additional limitation.



## Conclusion

The trend in polar moment of inertia was to decline to rib 3 or 4 and increase to rib 7. Polar moment of inertia was the most sensitive to the age of the cadaver. Bone volume and stiffness followed a similar trend. Anterior ribs had the lowest values for all the structural properties analyzed. Structural efficiency of lateral and posterior ribs varied little with rib level and cadaver age. Additionally, homogenized elastic modulus varied little between rib level and cadaver; however it was affected by anatomical position on the rib. Using an appropriate homogenized elastic modulus will improve solid homogenous FE models of ribs used in whole body FE models.

Future studies could analyze more ribs and sections further from the costal cartilage junction. Furthermore, evaluating the cortical rib compartment alone could provide an elastic modulus useful in hollow cross sectional models.

## Acknowledgements

Funding provided by the National Space Biomedical Research Institute through NASA NCC9-58. This project was made possible (in part) by support from the Office for Undergraduate Research at UNC-Chapel Hill.



THE UNIVERSITY  
of NORTH CAROLINA  
at CHAPEL HILL

NC STATE  
UNIVERSITY